The Influence of Lateral Interactions between Adsorbed Molecules on Adsorption Kinetics. A Statistical Rate Theory Approach

Tomasz Panczyk*

Group for Theoretical Problems of Adsorption, Institute of Catalysis and Surface Chemistry, Polish Academy of Sciences, ul. Niezapominajek 8, 30-239 Krakow, Poland

Pawel Szabelski

Department of Theoretical Chemistry, Faculty of Chemistry, UMCS, pl. Marii Curie-Sklodowskiej 3, Lublin 20-031, Poland

Received: February 11, 2003; In Final Form: April 3, 2003

The influence of lateral interactions between the adsorbed molecules is studied using the statistical rate theory (SRT). This approach makes it possible to introduce the interaction term into the kinetic equation in an easy and thermodynamically consistent way. The quasi-chemical approximation was applied to calculate the chemical potential of adsorbed molecules. The short-time behavior of the kinetic equation based on SRT is in agreement with experimental findings for the systems with lateral interactions. Moreover, the long-term behavior agrees with the equilibrium Langmuir isotherm combined with the quasi-chemical approximation. The experimental system, CO adsorption on Rh(100), was used for quantitative analysis; as a result, a good simultaneous description of equilibria and kinetics in this system was obtained.

I. Introduction

The theoretical description of adsorption/desorption kinetics is commonly based on the absolute rate theory (ART),[1] which was originally derived for the case of chemical reactions, as a method for calculating the rate constant. The rate of adsorption/desorption in the ART approach is described by

$$\frac{d\theta}{dt} = K_a p(1-\theta)^s \, e^{-(\epsilon_a/(kT))} - K_d \theta^s \, e^{-(\epsilon_d/(kT))} \qquad (1)$$

where θ is the fractional coverage of adsorption sites, s is the number of sites involved in an elementary adsorption/desorption process, t is time, p is the partial pressure of gas-phase adsorbate, T is absolute temperature, ϵ_a and ϵ_d are activation energies for adsorption and desorption, and K_a and K_d are the related constants.[1] Equation 1 is commonly called the Wigner−Polanyi equation for adsorption kinetics.

When $s = 1$ and $d\theta/dt = 0$, eq 1 yields the Langmuir adsorption isotherm

$$\theta^{(e)}(p,T) = \frac{Kp^{(e)} \exp\left(\frac{\epsilon}{kT}\right)}{1 + Kp^{(e)} \exp\left(\frac{\epsilon}{kT}\right)} \qquad (2)$$

where $K = K_a/K_d$ and $\epsilon = (\epsilon_d - \epsilon_a)$ and where the superscript (e) refers to equilibrium. Equation 1, with $s = 1$, describes what is commonly called "Langmuirian kinetics".

However, experimental data of adsorption/desorption kinetics rarely follow eq 1. This is especially true for the coverage dependence of experimental sticking probability data, which should be a linear function of θ as predicted by eq 1. As a result, many scientists started to use empirical equations (e.g., the Elovich, power law) to correlate experimental data. Others attempted various improvements of ART, introducing the concept of a precursor state.[2−4] This approach enabled an explanation of nonlinear behavior of sticking probability as a function of surface coverage. However, many additional simplifying assumptions had to be made. The major drawback in this case was an introduction of several parameters of which the theoretical calculation was practically impossible.

At the beginning of the 1980s, new theoretical approaches to adsorption/desorption kinetics appeared.[5−9] They related the kinetics of adsorption/desorption to the chemical potentials of the adsorbed and bulk-phase molecules. The most theoretically advanced is, however, the statistical rate theory (SRT) developed by Word and co-workers.[10,11]

In the recent publication,[12] Rudzinski and Panczyk reviewed such, mentioned above, different theoretical approaches to the kinetics of adsorption/desorption. In that work, it was also demonstrated that the kinetics of adsorption, even in the simple, energetically homogeneous system, depends on the experimental conditions at which the process is carried out. In the case of the ART approach, such effect cannot be observed.

The new SRT approach has been successfully used to describe a variety of interfacial phenomena.[10,11,13−29] In a recent series of papers Rudzinski and co-workers[30−39] also generalized the SRT approach to describe the kinetics of adsorption/desorption on/from energetically heterogeneous solid surfaces. These generalizations concern both the isothermal adsorption kinetics and the kinetics of thermal desorption. It was shown that the well-known empirical kinetic equations, such as the Elovich or the power law expressions, describe the kinetics of isothermal adsorption in systems in which the adsorption equilibria are described by well-known isotherm equations, the Temkin and

* To whom correspondence should be addressed. Mailing address: Department of Theoretical Chemistry, Faculty of Chemistry, UMCS, Pl. M. Sklodowskiej-Curie 3, 20−031 Lublin, Poland. Tel: +48 81 537 5620. Fax: +48 81 537 5685. E-mail: laibach@vega.umcs.lublin.pl.

10.1021/jp034354z CCC: $25.00
Published on Web 05/17/2003

the Freundlich equation, respectively. Moreover, a more general form of these kinetic equations was developed by taking rigorously into account both the adsorption and desorption terms and used to fit quantitatively experimental data reported in the literature.

The purpose of the present publication is to show how the lateral interactions between adsorbed molecules influence the adsorption kinetics. The SRT approach gives a very simple and thermodynamically consistent way of taking into account these effects. For the ART approach, it seems that the interactions in the adsorbed phase may influence only the kinetics of desorption; the adsorption term seems to be independent of the interaction parameters. Also the Kisliuk's[2] equation for the precursor-mediated sticking coefficient does not take into account these effects.

In this paper, we present model calculations showing qualitative behavior of the systems with attractive and repulsive interactions in the adsorbed layer. Also, a quantitative analysis of the adsorption kinetics of CO on Rh(100) is performed. The analysis indicates that the SRT approach provides a good simultaneous description of the kinetic and equilibrium properties of this system.

II. Kinetics of Adsorption without Lateral Interactions between the Adsorbed Molecules

The full rate expression developed from the SRT approach may be written as follows:

$$\frac{d\theta}{dt} = K'_{gs}\left[\exp\left(\frac{\mu_g - \mu_a}{kT}\right) - \exp\left(\frac{\mu_a - \mu_g}{kT}\right)\right] \tag{3}$$

where K'_{gs} is the equilibrium exchange rate, θ is the nonequilibrium surface coverage, and t is time. The parameter K'_{gs} is expressed as a function of the equilibrium surface coverage, $\theta^{(e)}$, and of the corresponding equilibrium pressure in the isolated system, $p^{(e)}$,[23]

$$K'_{gs} = K_{gs}(1 - \theta^{(e)})p^{(e)} \tag{4}$$

where K_{gs} is now only temperature-dependent parameter.

At quasi-equilibrium conditions, that is, when the chemical potential of the adsorbed molecules has the same value over entire surface, and for the Langmuir model of adsorption,

$$\mu_s = kT \ln \frac{\theta}{1-\theta} - kT \ln q^s \tag{5}$$

where q^s is the molecular partition function of the adsorbed molecules, commonly written as the following product,

$$q^s = q_0^s \exp\left(\frac{\epsilon}{kT}\right) \tag{6}$$

where ϵ is the adsorption potential that is well-known from equilibrium thermodynamics and q_0^s is the molecular partition function including all internal degrees of freedom of the adsorbed molecule except for ϵ. If we assume that the chemical potential of bulk phase may be expressed by

$$\mu_g = \mu_0^g + kT \ln p \tag{7}$$

where μ_0^g is the standard chemical potential of gas phase, then the SRT rate equation ($d\theta/dt$) takes the form

$$\frac{d\theta}{dt} = K_{gs}(1 - \theta^{(e)})p^{(e)}\left[Kp\frac{1-\theta}{\theta}\exp\left(\frac{\epsilon}{kT}\right) - \frac{1}{Kp}\frac{\theta}{1-\theta}\exp\left(-\frac{\epsilon}{kT}\right)\right] \tag{8}$$

where

$$K = q_0^s \exp\left(\frac{\mu_0^g}{kT}\right) \tag{9}$$

At equilibrium, when $(d\theta/dt) = 0$, one arrives at the Langmuir isotherm,

$$\theta^{(e)}(p,T) = \frac{Kp^{(e)}\exp(\epsilon/(kT))}{1 + Kp^{(e)}\exp(\epsilon/(kT))} \tag{10}$$

Equation 8 predicts the kinetics of adsorption in an isolated isothermal system, but it can also be applied to the systems for which the total number of molecules in the system changes with time.[24,25] The total number of molecules in the entire system is N, so we can write

$$N = N_s + N_b = \theta MS + \frac{pV}{kT} \tag{11}$$

where N_s is the number of adsorbed molecules, N_b is the number of molecules in the bulk phase, θ is the instantaneous (nonequilibrium) coverage of surface adsorption sites, M is the number of adsorption sites per unit of surface area, S is the geometrical area of the adsorbing surface, p is the instantaneous pressure of the bulk phase, and V is the volume of adsorption chamber. At any instant of time, the mass balance must be held,

$$\theta MS + \frac{pV}{kT} = \theta^{(e)}MS + \frac{p^{(e)}V}{kT} \tag{12}$$

The quantities $\theta^{(e)}$ and $p^{(e)}$ can be considered as hypothetical equilibrium values of pressure and coverage in an isolated system (consisting of N molecules), which would appear when the system reaches equilibrium.

Substituting isotherm eq 10 into eq 12, introducing the dimensionless parameter $\eta = V/(MSkTK\exp(\epsilon/(kT)))$ and rearranging, we obtain the following equation:

$$\theta(t) + K\,e^{\epsilon/(kT)}\,p\eta = \theta^{(e)} + \eta\frac{\theta^{(e)}}{1-\theta^{(e)}} \tag{13}$$

Looking at eq 13, we can consider some simplified limiting cases. When the parameter η takes high values, that is, the amount of the gas phase above the surface dominates strongly over the adsorbed portion, then $K\exp(\epsilon/(kT))\,p = \theta^{(e)}/(1-\theta^{(e)})$. Thus, the expression before the square bracket in eq 8 may be written as follows:

$$K_{gs}(1 - \theta^{(e)})p^{(e)} = K_{gs}\frac{p}{1 + K\,e^{\epsilon/(kT)}\,p} \tag{14}$$

In our previous publications, we called such systems *volume-dominated*.[12,36] It seems that the above case is most probable for high-pressure adsorption experiments.

Next, we consider the situation when the parameter η takes values close to zero. This means that the surface can accommodate many more molecules than bulk phase. Such situation takes place when the experiment is carried out at very low pressures of adsorbate.

Thus, in this case, $\theta = \theta^{(e)}$, and

$$K_{gs}(1 - \theta^{(e)})p^{(e)} = K_{gs}\frac{\theta}{K\,e^{\epsilon/(kT)}} \tag{15}$$

This system was also considered earlier work[12,36] and called *solid-dominated*.

In our previous papers, one more case was described. Namely, it was the *equilibrium-dominated* system.[12,36] Assuming that $\theta^{(e)} \approx \theta$ and $p^{(e)} \approx p$, one obtains

$$K_{gs}(1 - \theta^{(e)})p^{(e)} = K_{gs}(1 - \theta)p \tag{16}$$

Such situation is possible when the adsorption process consists of a series of steps. During each step, the pressure is increased and the system is allowed to reach an instantaneous equilibrium. Next, the pressure is increased again until it reaches the final value p. When $\theta^{(e)}$ is small, the equilibrium-dominated system becomes identical with the volume-dominated system, and then one can use eq 16 instead of eq 14.

The equilibrium-dominated model gives very simple, compact expressions describing the kinetics of adsorption on energetically heterogeneous surfaces.[35,37−39] These expressions were successfully applied to fit quantitatively experimental data of adsorption kinetics in various experimental systems.

From eq 13, one can easily develop an expression describing $\theta^{(e)}$ as a function of nonequilibrium coverage and pressure,

$$\theta^{(e)}(\theta,p) = \frac{1}{2} + \frac{\eta(1 + K\,e^{\epsilon/(kT)}\,p)}{2} + \frac{\theta}{2} - \frac{1}{2}\sqrt{(1 + \eta(1 + K\,e^{\epsilon/(kT)}\,p) + \theta)^2 - 4(\eta K\,e^{\epsilon/(kT)}\,p + \theta)} \tag{17}$$

The above equation can be directly inserted into eq 8, remembering that $p^{(e)}$ is a function of $\theta^{(e)}$ via relation 10.

The possible limiting cases of eq 8 mentioned above have already been analyzed in our previous papers.[12,36] They predict correctly the shape of the experimental kinetic curves published in the literature, and they prove that the experimental conditions at which the adsorption process is carried out has a significant influence on adsorption kinetics. The essential feature of the SRT is that it involves a precise distinction between equilibrium and nonequilibrium values of coverage and pressure. On the basis of eq 1, one often treat the pressure p as being equal to or very close to equilibrium pressure.

III. Kinetics of Adsorption with Lateral Interactions between Adsorbed Molecules

In the theories of adsorption equilibria, two analytical approaches are generally known, which enable taking into account the effects of interactions between adsorbed molecules. The simplest method is the mean-field approximation (MFA).[40] According to the mean-field approximation, chemical potential of adsorbed molecules is given by

$$\mu_a = kT \ln \frac{\theta}{q^s(1 - \theta)} + cw\theta \tag{18}$$

where c is the coordination number and w is the interaction energy between two molecules adsorbed on adjacent sites. The critical temperature for the two-dimensional phase transition lattice gas ⇔ dense ordered phase is described by

$$T_c = -\frac{cw}{4k} \tag{19}$$

So, the problem of taking into consideration the interactions between the adsorbed molecules reduces only to adding to adsorption potential ϵ in eq 8 an additional configurational energy term, $\epsilon_{in} = -cw\theta$.

The second, more accurate approximation is the well-known quasi-chemical approximation (QCA).[40] In this case, the chemical potential of adsorbed molecules takes more complicated but more accurate form,

$$\mu_a = kT \ln \frac{\theta}{q(1 - \theta)} + \frac{cw}{2} + \frac{ckT}{2} \ln \frac{(f - 1 + 2\theta)(1 - \theta)}{(f + 1 - 2\theta)\theta} \tag{20}$$

where

$$f = \left\{1 - 4\theta(1 - \theta)\left[1 - \exp\left(-\frac{w}{kT}\right)\right]\right\}^{1/2} \tag{21}$$

Now, the critical temperature predicted by the quasi-chemical approximation is described by

$$T_c = \frac{w}{2k \ln \frac{c - 2}{c}} \tag{22}$$

which is slightly higher than the exact critical temperature for the two-dimensional square lattice: $w/(2k\,\ln(\sqrt{2} - 1))$.[40] Although the exact analytical solution for the square lattice with nearest-neighbors interactions is known in the literature, we confine ourselves to the approximate solution because of its simplicity and quite good accuracy when the system is not very close to phase transition.

In the case of the quasi-chemical approximation, the additional energy term has to be added to ϵ, that is,

$$\epsilon_{in} = -\frac{cw}{2} - \frac{ckT}{2} \ln \frac{(f - 1 + 2\theta)(1 - \theta)}{(f + 1 - 2\theta)\theta} \tag{23}$$

Quasi-chemical approximation does not give a detailed insight into all important and interesting phenomena that occur in real systems with lateral interaction (e.g., nucleation, growth phenomena, or ordering). Of course, one can use more sophisticated methods for calculation of the chemical potential of the adsorbed phase (e.g., DFT, computer simulations, transfer matrix method), and this can be the subject of our future research. However, as shown by Ceyrolles et al.,[41] even the simple MFA approximation gives results close to those obtained by Monte Carlo simulations of adsorption kinetics provided that the system is not very close to phase transition.

In this paper, we are going to examine whether the SRT approach is able to recover the adsorption kinetics with lateral interactions in a model adsorption system. As we show in the next sections, the QCA combined with the SRT describes correctly both the equilibria and kinetics of CO adsorption on Rh(100) surface.

In the case of interactions between adsorbed molecules, eqs 14−16 cannot be applied as they stand. The equilibrium coverage and pressure have to be calculated from the related isotherm equation including the appropriate interaction term, here eq 23. One can again introduce the limiting cases, volume, solid, or equilibrium, and the equilibrium exchange rate has to be calculated directly from eq 4. Additionally, it is possible to treat an adsorption system as intermediate between solid and volume, as it was done in eq 12, but now this equation must be

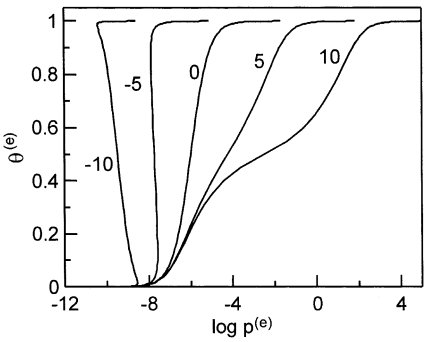

Figure 1. Examples of adsorption isotherms calculated using QCA approach and assuming the following values of the parameters: $\epsilon = 100$ kJ/mol; $T = 300$ K; $K = 3.87 \times 10^{-12}$ Pa^{-1}; $c = 4$. The values of the interaction parameter w are indicated in the figure (in kJ/mol).

solved numerically to obtain the values $\theta^{(e)}$ and $p^{(e)}$ for the given values of θ and p.

IV. Model Calculations and Discussion

Equation 8 derived in the previous section has to be solved numerically to obtain the function $\theta(t)$, which is often used to describe the kinetics of adsorption process in terms of the uptake curve. So, we have to assume certain values of the parameters, which will create the associated model system. Its examination will, thus, give us some general information about the possible role of interactions in the kinetics of adsorption.

Let us assume that the adsorption system consists of ideal gas phase and the surface is viewed as a square lattice of adsorption sites. In this case, the coordination number $c = 4$ and all of the adsorption sites have the same adsorption potential, ϵ. Let us accept that $\epsilon = 100$ kJ/mol, a value that is quite typical for chemisorption. Next, we have to assume certain values of the parameters K and K_{gs}. The parameter K is only temperature-dependent, and its dependence on temperature is not very strong compared to the term $\exp(\epsilon/(kT))$. We choose the value of K in such a way that for $p = 10^{-6}$ Pa and for $w = 0$ (no interactions) the equilibrium coverage would be $^1/_2$. The required value of K can be calculated from the equilibrium adsorption isotherm (eq 10). At temperature $T = 300$ K, K is assumed to be equal to 3.87×10^{-12} Pa.

When we combine the Langmuir adsorption isotherm (eq 10) with the QCA interaction term (eq 23), we can calculate an adsorption isotherm for certain values of interaction energy between nearest neighbors. A few examples of such adsorption isotherms are plotted in Figure 1. We stress that the values of the parameters accepted in this section do not correspond with any real adsorption system. The shape of adsorption isotherms describes qualitatively the essential physical phenomena that occur when the lateral interactions in adsorbed phase play a significant role. For the strong attractive interactions (negative values of w), one observes S-shaped adsorption profiles. This indicates an existence of two-dimensional phase transitions. The location of the point of phase transition can be estimated using the Maxwell construction. Repulsive interactions (positive values of w) cause a plateau to appear when $\theta^{(e)} = ^1/_2$. This effect can be attributed to the ordering of adsorbed phase.

Next, we need to assume a certain reasonable value of the parameter K_{gs}. Because the term K'_{gs}, by definition, describes the exchange rate between phases at equilibrium, we can calculate K_{gs} from an equation describing the number of collisions of gas molecules with flat surface, that is,

$$K_{gs} = \frac{1}{M\sqrt{2\pi mkT}} \tag{24}$$

The parameter M was introduced into eq 24 because K'_{gs} has to be expressed in ML/s.

Assuming that $M = 10^{19}$ sites/m^2, $m = 28$ g/mol, and $T = 300$ K, we find that $K_{gs} = 2874$ Pa^{-1} s^{-1}. The parameter K_{gs} describes how fast is the adsorption process. The higher its value the faster equilibrium state is reached. We can see that K_{gs} is expressed in reversed exposure units. This is in agreement with experimental observation that the higher is exposure the faster is adsorption.

The parameter η in eq 13 can take values from zero up to very high positive values. Looking at the definition of the parameter η, we can make a rough estimation of its value. For the accepted values of the parameters K, ϵ, and M, we have $\eta = (V/S)2.4 \times 10^{-5}$, so if we assume that $V = 5$ dm^3 and $S = 0.05$ cm^2, then $\eta = 0.024$.

Figure 2 shows a few results of the calculation carried out without lateral interactions in adsorbed phase for different values of parameter η. Also the limiting versions of eq 8, that is, solid-, volume-, and equilibrium-dominated, are plotted to emphasize their basic properties. From Figure 2, it follows that for η greater than 1 the system is already volume-dominated. Noticeable changes in the kinetic curves appear for $\eta < 1$ until it reaches the value ca. 10^{-3}. A smaller value of η generates the kinetic curves that are identical to those obtained for the solid-dominated system. Our estimation of η suggests that for the accepted values of the parameters the system is intermediate between volume- and solid-dominated ones.

However, the calculation of the parameter η may be difficult because the volume, V, has the sense of thermodynamic volume of an isolated system to which the SRT can be applied. The volume of adsorption chamber may, in general, not be identical with thermodynamic volume, V. So, it is reasonable to treat η as a best-fit parameter or to use the limiting cases described above, when possible.

From the analysis of Figure 2, it follows that, regardless of the value of η, the kinetic curve will always lie between the solid- and volume-dominated curve. The equilibrium-dominated curve is somewhat different from the volume-dominated one, but it represents a special case of realization of an experiment. Thus, further analysis of the influence of lateral interactions on the adsorption kinetics will be focused on the volume- and solid-dominated versions of eq 8.

Figure 3 presents the set of kinetic curves showing how the interactions between the adsorbed molecules affect the adsorption kinetics. The solid lines in both parts of Figure 3 represent the case when no interactions between adsorbed molecules exist, that is, for $w = 0$. The dashed lines correspond with the following values of the interaction parameter w: -0.5, -1, -2, -3, and -4 kJ/mol, as indicated in the caption of Figure 3. The negative values of w denote the presence of attractive interactions between adsorbed molecules. The dotted lines in Figure 3 are plotted for the positive values of the parameter w: 0.5, 1, 2, 3, and 4 kJ/mol. This is the case of repulsive interactions in the adsorbed layer.

As it follows from Figure 3, the behavior of volume- and solid-dominated systems with interactions are much different from each other. Because these are only limiting, extreme cases, one can also examine intermediate systems of which the features would be intermediate as well. Apart from the quantitative differences between volume- and solid-dominated system, one can notice also a general, qualitative similarity between them.

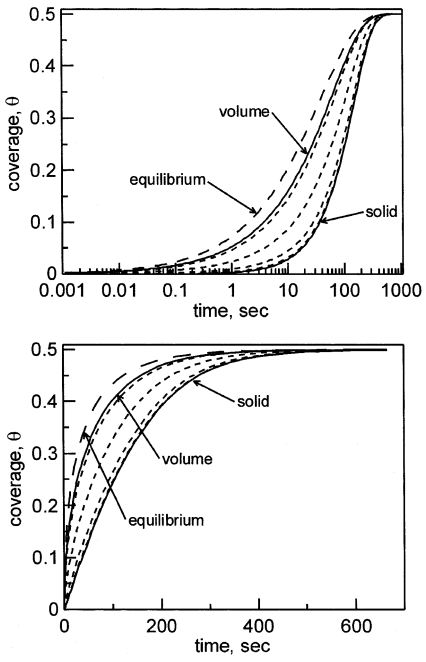

Figure 2. The integral kinetic curves of adsorption obtained by numerical solution of eq 8 with the parameters $K = 3.87 \times 10^{-12}$ Pa^{-1}, $K_{gs} = 2874$ Pa^{-1} s^{-1}, $\epsilon = 100$ kJ/mol, $T = 300$ K. In this case, the interaction parameter w was assumed to be zero, that is, no interactions are present in the adsorbed layer. The solid lines in both parts of Figure 2 correspond with volume- and solid-dominated cases; the dashed line represents the equilibrium-dominated case. The dotted lines represent intermediate states between solid- and volume-dominated cases, and the parameter η takes the values (from solid- to volume-dominated cases) 10^{-3}, 10^{-2}, 10^{-1}, and 1.

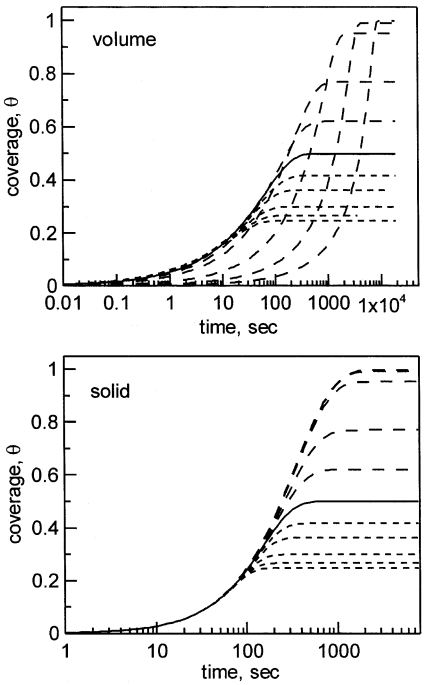

Figure 3. The influence of lateral interactions on the adsorption kinetics. The dashed lines (− − −) represent the case of attractive interactions, and the parameter w takes the values −0.5, −1, −2, −3, and −4 kJ/mol (from the bottom to the top curve). The solid line is drawn for the case $w = 0$, that is, no interactions are present. Repulsive interactions are represented by dotted lines (- - -), where the parameter w takes the values 0.5, 1, 2, 3, and 4 kJ/mol (from the top to the bottom curve). All of the calculations were carried out assuming that the coordination parameter $c = 4$, $p = 10^{-6}$ Pa, $K = 3.87 \times 10^{-12}$ Pa^{-1}, $K_{gs} = 2874$ Pa^{-1} s^{-1}, and $\epsilon = 100$ kJ/mol.

Both models reproduce qualitatively essential features of systems with lateral interactions.

For the growing strength of attractive interactions, one observes slower and slower adsorption, followed next by rapid increase of coverage near equilibrium. It is most clearly seen for the volume-dominated system. Such effect can be attributed to an island formation. At equilibrium, one observes then S-shaped adsorption profiles. In the case of a solid-dominated system, the time during which the equilibrium state is reached also increases with growing strength of attractive interactions, but for quite large value of coverage (ca. 0.2), interactions seem to play a negligible role. Also the increase of coverage near equilibrium is not as rapid as in the case of the volume-dominated system.

In the case of repulsive interactions, predictions of both models become more similar. One observes a negligible effect of interactions for the coverages up to 0.2. Such effect is easy to understand because in the case of repulsive interactions the adsorbed layer orders to minimize the repulsion. In consequence, the repulsions do not affect the kinetic curve (also sticking probability) until the coverage is quite large. Moreover, for the volume-dominated system, one observes even an acceleration of adsorption for strong repulsive interactions. This effect may be connected with speeding up energy accommodation.

The long-term behavior of both systems is identical. For high values of t ($t \rightarrow \infty$) the equilibrium coverage predicted by both models, solid- and volume-dominated, matches the value of equilibrium coverage, $\theta^{(e)}(T,p^{(e)},w)$, calculated from the Langmuir isotherm combined with the QCA interaction term. For negative values of w, one observes a strong increase of equilibrium coverage, whereas for positive values of w, the decrease of equilibrium coverage is much less.

In the adsorption equilibria, the presence of attractive interactions in the adsorbed layer leads to the existence of two-dimensional phase transitions. Such phase transitions are complex phenomena, and advanced theoretical methods are needed to treat them correctly. Particularly, when close to phase transition, the results obtained using the QCA should be treated with caution. It is generally known that the QCA, which accounts only for the interactions between nearest neighbors, introduces errors mostly in the region of the phase transition. First of all, the location of the phase transition point will be slightly different than that obtained for the correct solution. But the other qualitative features of the system should be similar, so qualitatively, our model should give reasonable results also in this critical region. However, a precise estimation of the errors introduced by applying the QCA in our model can be made only by a direct comparison with the exact or less approximate results. Such results can be obtained by applying more advanced techniques, for example, Monte Carlo simulations. Nevertheless, we are going to make a first insight into the essential features of SRT, which seems to be a useful tool for the description of the adsorption kinetics with lateral interactions between adsorbed molecules. Thus, for the sake of simplicity, we still confine ourselves to the QCA approximation.

Because, in the case of adsorption kinetics, coverage depends at least on two independent variables (pressure and time), we decided to prepare three-dimensional graphs to see the simultaneous influence of these parameters on the coverage. In Figure 4, we present the dependence of the coverage as a function of pressure and time for a selected set of the parameters. The assumed value of the interaction parameter w is −3 kJ/mol. The critical temperature predicted by the quasi-chemical ap-

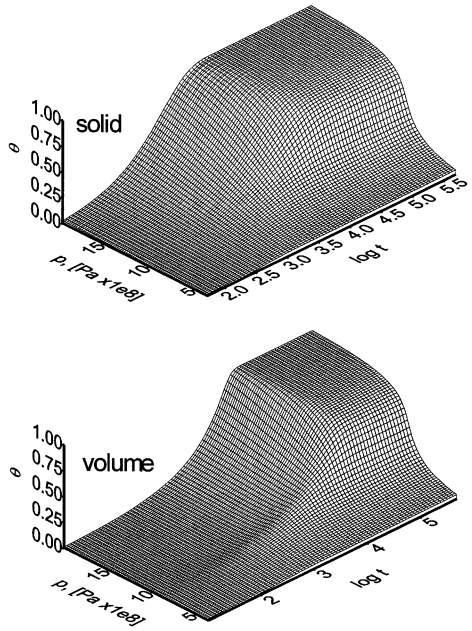

Figure 4. The surface $\theta(p,t)$ calculated for the following set of parameters: $w = -3$ kJ/mol; $c = 4$; $K = 3.87 \times 10^{-12}$ Pa^{-1}; $K_{gs} = 2874$ Pa^{-1} s^{-1}; $\epsilon = 100$ kJ/mol; $T = 300$ K. The critical temperature predicted by the quasi-chemical approximation $T_c = 260.29$ K.

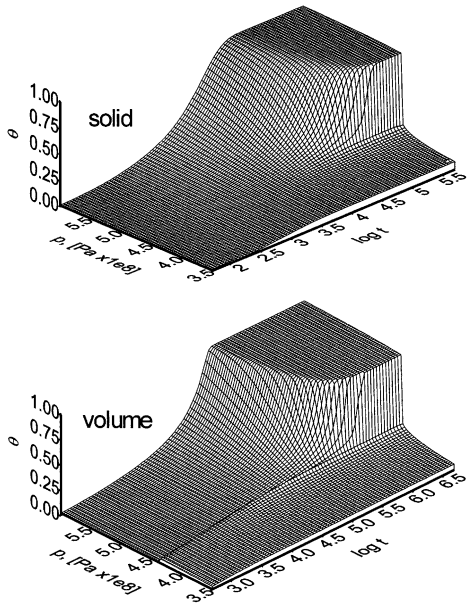

Figure 5. The surface $\theta(p,t)$ for the parameter w ($w = -4$ kJ/mol) chosen in such a way that the critical temperature predicted by QCA ($T_c = 347.05$ K) is higher than assumed in calculations, $T = 300$ K. The other parameters are $c = 4$; $K = 3.87 \times 10^{-12}$ Pa^{-1}; $K_{gs} = 2874$ Pa^{-1} s^{-1}; $\epsilon = 100$ kJ/mol.

proximation for this case is 260.29 K, but the temperature assumed during the calculation is 300 K. In these conditions, any phase transition cannot be observed, and as expected, we can see a smooth surface for both solid- and volume-dominated systems. For the solid-dominated system, the increase of θ is monotonic with increasing pressure and time. For a certain value of p, we can see quite rapid increase of θ for long times. However, this increase is continuous, and for shorter times it slowly disappears.

The volume-dominated system represents somewhat different behavior for short times. When the time does not exceed ca. 10^4 s, a small maximum can be observed on the curve $\theta(p,t_{fix})$ (t_{fix} = fixed time). This effect can be attributed to the nucleation and growth phenomenon. For small pressures, the above effects do not occur and adsorption kinetics proceeds as if there would not exist any interactions. Accordingly at higher pressures, however, the adsorption is slower and slower, and for long times, it accelerates considerably.

We stress again that the volume- and solid-dominated systems are extreme cases. Of course, real systems are expected to be intermediate between these two limiting cases. However, it is also possible that some of the real systems would resemble solid- or volume-dominated systems as well. It is interesting that the construction of experimental setup has such important influence on the behavior of adsorption kinetics. This effect can be easily noticed with the help of the SRT approach.

In Figure 5, an analogous graph is presented but the interaction parameter w is higher ($w = -4$ kJ/mol). Now, the critical temperature calculated from eq 22 is $T_c = 347.05$ K. Thus, as expected, we can see a sudden jump in the surface $\theta(p,T)$ for a certain value of $p = p_{tr}$ ($p_{tr} = 4.358 \times 10^{-8}$ Pa). In this case, the behavior of volume- and solid-dominated systems is much different than before, when the temperature was higher than the critical temperature. However, for long times, both systems also match the Langmuir equilibrium isotherm combined with the QCA interaction term and produce a jump in the coverage for $p = p_{tr}$. For shorter times (less than 10^4 s), the solid-dominated system does not reveal any discontinuities in the function $\theta(p,t_{fix})$. For pressures greater than p_{tr}, the equilibrium state is reached later than for the pressures lower than p_{tr}. When the system goes from $p > p_{tr}$ toward p_{tr}, equilibrium is reached later and later, and at the point $p = p_{tr}$, the equilibrium coverage seems to be indeterminate and the time needed for equilibration is infinite.

The general features of the volume-dominated system are very similar to those of the solid-dominated one for long times, but for short times, they are much different. The striking feature of the volume-dominated system is the discontinuity of the function $\theta(p,t_{fix})$ for all values of t_{fix}. For short times, the function $\theta(p,t_{fix})$ is increasing with increasing p, but when the pressure exceeds p_{tr}, the coverage rapidly drops down to a very small value. For pressures higher than p_{tr}, the adsorption is very slow and grows rapidly near equilibrium.

Before the phase transition ($p < p_{tr}$), the time needed for equilibration in both systems is in the range 10^3-10^4 s, but when $p > p_{tr}$, this time grows to the value about 10^5 s for the solid-dominated system but for volume-dominated it is even higher, ca. 10^6 s.

It is interesting that the kinetic curves for a fixed value of p are always continuous, before the phase transition and behind, as well. For the solid-dominated system, the kinetic curve for $p = p_{tr}$ is also continuous up to a certain value of time, which precise calculation was not possible. On the contrary, the kinetic curve at $p = p_{tr}$ for the volume-dominated system does not exist even for very short times.

In Figure 6, we show cross sections of the surfaces $\theta(p,t)$ for both systems done for fixed values of time, t_{fix}. Also, the equilibrium adsorption isotherm is plotted to see how the long time behavior of our kinetic equations match the full equilibrium predictions. From the analysis of Figure 6, it follows that the kinetic equations for both systems fully agree with equilibrium adsorption isotherm for long times. However, it is clear that the kinetic equations predict that the system passes through metastable states, and the location of the pressure under which the phase transition occurs (p_{tr}) is not precisely determined. This result is similar to that obtained with Monte Carlo simulations

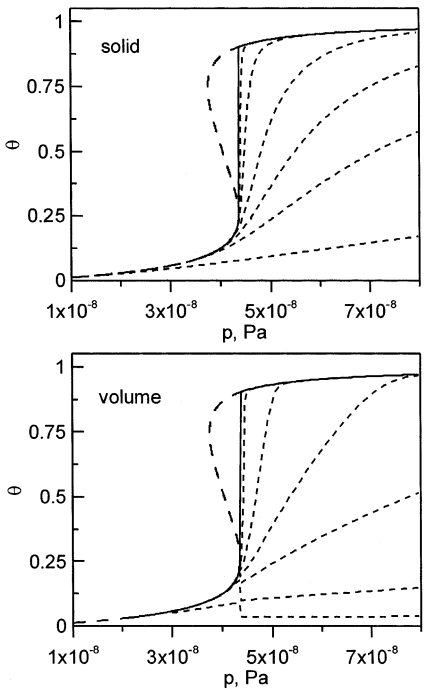

Figure 6. The comparison between the equilibrium adsorption isotherm, calculated using the QCA approximation (dashed line), and the equilibrium value of $\theta(p,t)$ for both systems (solid line), calculated from eq 8, that is, when $t \rightarrow \infty$. The dotted lines are the cross sections of the surfaces $\theta(p,t)$ from Figure 5 for fixed times, t_{fix}. For the solid-dominated system, the following values of t_{fix} were accepted: 10^3, 5×10^3, 10^4, 2×10^4, 5×10^4, and 10^5 s (from the bottom to the top curve). For the volume-dominated systems, the values of t_{fix} were the following: 10^3, 10^4, 5×10^4, 10^5, 2×10^5, and 5×10^5 s (from the bottom to the top curve).

of equilibrium adsorption isotherms. However, from equilibrium properties of the system (see eqs 10, 20, and 21), it is known that the pressure under which phase transition occurs should be $p_{tr} = p^{(e)}(\theta^{(e)}=0.5)$.

For the solid-dominated system, we observe that the curves $\theta(p,t_{fix})$ are always continuous. The discontinuity appears only at full equilibrium (solid line in Figure 6). Even for times not very far from equilibrium, the curves $\theta(p,t_{fix})$ are smooth but they become steeper and steeper. The volume-dominated system reveals much different behavior. For short times, one observes a jump in the curve $\theta(p,t_{fix})$. When time incereases this jump becomes smaller and smaller, and for quite long times, it reduces to a point. At this point, at equilibrium, one observes the well-known jump in the equilibrium adsorption isotherm.

The model investigations presented here show that the influence of lateral interactions on the adsorption kinetics is interesting and needs detailed investigations based on more advanced theoretical methods. On the basis of SRT, it is quite straightforward because the correctness of this approach is, first of all, based on the accuracy of estimation of chemical potential of adsorbed molecules. In the next section, we present an analysis of one experimental system with lateral interactions, using the SRT approach and QCA approximation.

V. CO Adsorption on Rh(100)

The system CO/Rh(100) has been widely studied in the literature, and all essential properties of CO adsorbed on a rhodium single-crystal plane (100) have been resolved. It is generally known that at room temperatures CO adsorbs molecularly and up to 0.5 ML coverage it is coordinated linearly giving a c(2×2) overlayer structure. For higher coverages, from 0.5 up to 0.75 ML, also a bridged state appears and p($4\sqrt{2} \times \sqrt{2}$)R45° pattern is observed, which corresponds with the saturation coverage at room temperature, 0.75 ML.[42] Activation energy for desorption at zero coverage ranges from ~130 to ~140 kJ/mol and drops to ~80 kJ/mol at saturation.[42−45] On the other hand, there is no information about the existence of activation energy for adsorption in this system.

The isosteric heat of adsorption data reported by Kose et al.[43] indicate the existence of strong repulsive interactions in the adsorbed phase. The sticking probability curve suggests that the precursor-mediated adsorption kinetics exist.[43] De Jong and Niemantsverdriet have published the uptake curve for the system CO/Rh(100) measured at the temperature 300 K.[42] With the help of the above-mentioned experimental data, we will be able to find some important parameters needed in the SRT equation.

The starting point in the SRT approach is the determination of chemical potentials of gas and adsorbed phases. For the gas phase, it is a very simple task because the gas pressures at which the kinetics and heats of adsorption were measured are very low, so it is reasonable to use the classical equation for the chemical potential of an ideal diatomic molecule:

$$\frac{\mu_g}{kT} = -\ln\left[\left(\frac{2\pi(m_1+m_2)kT}{h^2}\right)^{3/2} kT\right] - \ln\frac{T}{\Theta_{rot}} + \ln\left[1-\exp\left(-\frac{\Theta_{osc}}{T}\right)\right] - \frac{D_0}{kT} + \ln p^{(e)} \quad (25)$$

where m_1 and m_2 are the masses of oxygen and carbon atoms and Θ_{rot} and Θ_{osc} are the characteristic temperature for rotation and oscillation, respectively. D_0 is the dissociation energy of the CO molecule. All of the molecular parameters for CO are available in the literature: $\Theta_{rot} = 2.77$ K, $\Theta_{osc} = 3070$ K, and $D_0 = 9.14$ eV.[40]

The state of CO adsorbed on Rh(100) can be modeled as a single harmonic oscillator for coverages up to 0.5 ML. The IR spectra reported by de Jong and Niemantsverdriet show a single band of linearly adsorbed CO when the coverage does not exceed 0.5 ML.[42] However, for coverages higher than 0.5 ML, there appears a second band corresponding to bridged states, but the peak characteristic for linear CO is dominant for all coverages. So, we assume that a single harmonic oscillator model for CO adsorbed on Rh(100) is sufficient as a first approximation.

As follows from the IR spectra, the frequency of oscillation of the CO molecule changes with coverage approximately linearly. To take into account the increase of frequency of oscillation with increasing coverage, we used in the calculations a linear approximation of the wavenumber as a function of coverage. This approximation is shown in Figure 7.

The chemical potential of the adsorbed molecule will, thus, be given by the following equation:

$$\frac{\mu_a}{kT} = \ln\frac{\theta}{\theta_M-\theta} - \ln\left[q_z(\theta)\exp\left(\frac{\epsilon}{kT}\right)\right] - \ln {q_x}^2 + \frac{cw}{2kT} + \frac{c}{2}\ln\frac{(f-1+2\theta)(1-\theta)}{(f+1-2\theta)\theta} \quad (26)$$

where the QCA interaction term has been added. The $q_z(\theta)$ function is the coverage-dependent partition function of a harmonic oscillator with the frequency of oscillation corresponding to linearly adsorbed CO molecules, given by the linear function in Figure 7.

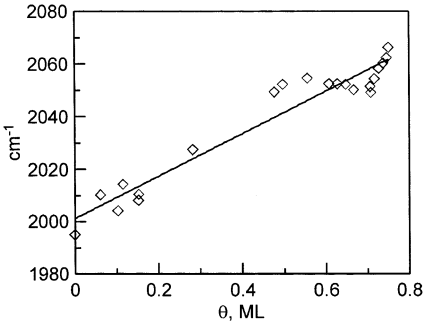

Figure 7. The experimental relationship between wavenumber of linearly adsorbed CO and the coverage. The linear reggression was performed to obtain analytical representation of this relation, after de Jong and Niemantsverdriet.[42]

$$q_z(\theta) = \frac{\exp\left(\frac{h\nu_z(\theta)}{2kT}\right)}{\exp\left(\frac{h\nu_z(\theta)}{kT}\right) - 1} \tag{27}$$

The θ_M parameter is the saturation coverage equal to 0.75 ML,[42] whereas q_x is the partition function for the horizontal vibrations of the adsorbed CO molecule. We assumed that q_x has the form of eq 27 but the frequency, ν_x, is constant now. Further, we assumed that the partition functions of horizontal oscillations in the x and y direction are the same, so the q_x in eq 26 is squared. Unfortunately, no information about the value of ν_x is available, also the value of the other spectroscopically inactive degrees of freedom of the adsorbed CO molecule are unknown. So, we will treat the frequency ν_x as a best-fit parameter, taking into account (to some extent) the neglected or unknown properties of CO adsorbed on Rh(100). The quantity ϵ in eq 26 is the well-known adsorption potential, which can be identified here with the activation energy for desorption.

The equilibrium adsorption isotherm for this system can be easily calculated and is given by the following equation:

$$\ln p^{(e)} = \ln \frac{\theta^{(e)}}{\theta_M - \theta^{(e)}} - \ln\left[q_z(\theta^{(e)}) \exp\left(\frac{\epsilon}{kT}\right)\right] + \frac{cw}{2kT} + \frac{c}{2} \ln \frac{(f - 1 + 2\theta^{(e)})(1 - \theta^{(e)})}{(f + 1 - 2\theta^{(e)})\theta^{(e)}} - \ln q_x^2 + \ln\left[\left(\frac{2\pi(m_1 + m_2)kT}{h^2}\right)^{3/2} kT\right] + \ln \frac{T}{\Theta_{rot}} - \ln\left[1 - \exp\left(-\frac{\Theta_{osc}}{T}\right)\right] + \frac{D_0}{kT} \tag{28}$$

From eq 28, one can easily calculate the isosteric heat of adsorption as a function of coverage,

$$Q_{st}(\theta) = -k\left(\frac{\partial \ln p}{\partial \frac{1}{T}}\right)_\theta = \epsilon - h\nu_x \operatorname{ctgh}\left(\frac{h\nu_x}{2kT}\right) - D_0 + \frac{k\Theta_{osc}}{\exp\left(\frac{\Theta_{osc}}{T}\right) - 1} + \frac{7}{2}kT - \frac{cw}{2} - \frac{1}{2}h\nu_z(\theta) \operatorname{ctgh}\left(\frac{h\nu_z(\theta)}{2kT}\right) + \frac{cw(1 - 2\theta)}{2\sqrt{1 - 4\theta(1 - \theta)\left(1 - \exp\left(-\frac{w}{kT}\right)\right)}} \tag{29}$$

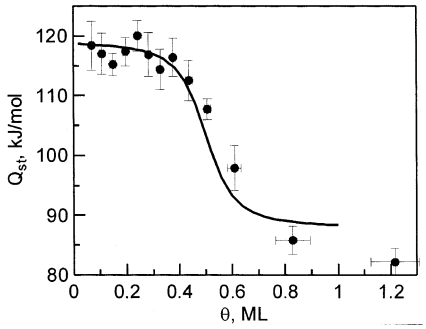

Figure 8. The result of fitting of the experimental data for the isosteric heat of adsorption in the system CO/Rh(100) reported by Kose et al.[43] The values of the parameters are collected in Table 1.

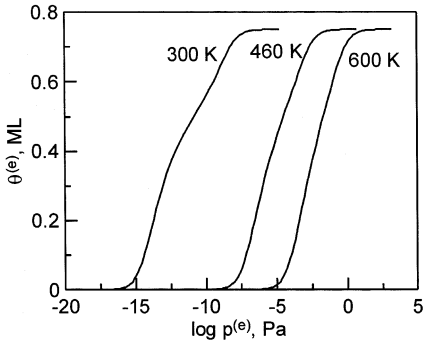

Figure 9. The equilibrium adsorption isotherms for the system CO/Rh(100) calculated from eq 28 and using the best-fit parameters collected in Table 1.

TABLE 1: The Values of the Parameters Found While Fitting the Isosteric Heat of Adsorption Data and Fulfilling Certain Features of the Equilibrium Adsorption Isotherm

ϵ [kJ/mol]	w [kJ/mol]	ν_x [Hz]
126.9	7.49	10^9

In eqs 28 and 29, there are three unknown parameters: ϵ, ν_x, and w. The best way of finding them would be simultaneous fitting of the equilibrium adsorption isotherm and the isosteric heat of adsorption for one certain set of these three parameters. Unfortunately, there is no available data for equilibrium adsorption isotherm for this system because of experimental difficulties met in that kind of experiment. Only some general features of adsorption isotherm can be deduced from the reported results. Namely, the adsorption isotherm should reach the saturation at the pressure about 10^{-6} Pa;[42] at the same time, it should give a negligible equilibrium coverage at temperatures about 600 K because the thermodesorption spectra fall down to zero signal at the temperatures 550−600 K.[42] Wei et al.[46] reported the desorption curves at the temperature 460 K for the system CO/Rh(100), and one can see that at this temperature the equilibrium coverage is close to zero (the background pressure applied in this experiment was $< 2 \times 10^{-10}$ Torr).

So, remembering about the above essential features of equilibrium adsorption isotherm and having at disposal the isosteric heat of adsorption data reported by Kose et al.,[43] we found the values of the parameters of interest. The result of fitting the isosteric heat of adsorption is shown in Figure 8, whereas a few samples of equilibrium adsorption isotherms for the system CO/Rh(100) are shown in Figure 9. The values of the parameters found are collected in Table 1. From Figure 8, it follows that eq 29 is satisfactory in describing the coverage dependence of isosteric heat of adsorption data for this system. For the coveargres up to 0.5 ML, it is even very good, but for

higher coverages some discrepancies appear. They are due, to some extent, to the simplified adsorption mechanism assumed by us for this coverage region. However, also the experimental data for the coverages higher than ca. 0.6 ML are uncertain. Kose et al. call their coverage "apparent coverage" because the experimental technique that they applied is not able to measure the absolute coverage when close to saturation. However, the authors assure that for the coverages at which the heat of adsorption is ≥100 kJ/mol, the coverage scale is accurate. Thus, the last two points in Figure 8 should lie, in fact, before the saturation coverage, that is, 0.75 ML.

The adsorption isotherms calculated from eq 28 and plotted in Figure 9 also show a correct behavior and follow the above-mentioned conditions, which can be deduced from the literature data for the adsorption of CO on Rh(100).

The value of the activation energy for desorption (adsorption potential) ϵ for the zero coverage limit agrees well with the values reported in the literature (130−140 kJ/mol) and obtained mainly from the thermodesorption experiments.[42,44−46] However, the initial heat of adsorption reported by Kose is 118 kJ/mol (Figure 8). Note that this is not a real disagreement because the heat of adsorption and the activation energy for desorption cannot be treated as the same quantities, as a rule.

The strength of interaction between the nearest neighbors, w, is slightly lower than the value found by Kose et al. during the Monte Carlo simulations of their experimental heat of adsorption. This may be attributed to the use of QCA approach, which takes into account only the nearest neighbors interactions. Kose et al.[43] introduced also the next-nearest and next-next-nearest neighbors interactions in the MC simulations, and as it is expected, their results better agree with experimental data than our simple equation based on the use of the QCA approach.

The frequency of horizontal oscillations, ν_x, was found to be 10^9 Hz; however, it should not be identified with the real frequency. This value is only effective because of the limited number of factors taken into account during the derivation of eqs 28 and 29.

The SRT rate equation for the system CO/Rh(100) can be derived from eq 3. For this particular system, eq 3 takes the following form:

$$\frac{d\theta}{dt} = K'_{gs}\left[K(T)q_z(T,\theta)\, e^{(\epsilon + \epsilon_{in}(\theta))/(kT)}\, p\frac{\theta_M - \theta}{\theta} - \frac{1}{K(T)q_z(T,\theta)p}\, e^{-(\epsilon + \epsilon_{in}(\theta))/(kT)}\frac{\theta}{\theta_M - \theta}\right] \quad (30)$$

where $\epsilon_{in}(\theta)$ is given by eq 23 whereas $K(T)$ is expressed as

$$K(T) = \frac{\left(1 - \exp\left(-\frac{\Theta_{osc}}{T}\right)\right)\exp\left(-\frac{D_0}{kT}\right)q_x{}^2\Theta_{rot}}{\left(\frac{2\pi(m_1 + m_2)kT}{h^2}\right)^{3/2}kT^2} \quad (31)$$

The equilibrium exchange rate K'_{gs} for this system may be calculated from the following equation:

$$K'_{gs} = \frac{p^{(e)}}{M\sqrt{2\pi(m_1 + m_2)kT}}(\theta_M - \theta^{(e)}) \quad (32)$$

because the considered adsorbing surface is flat. The unit of K'_{gs} is ML/sec.

Proper calculation of K'_{gs} needs a detailed analysis of the conditions at which the experiment has been carried out. We chose for an analysis the uptake curve reported by de Jong and Niemantsverdriet.[42] The experimental procedure that they applied was the following. When the crystal surface was suitably cleaned, the gas exposure was made by back-filling the experimental chamber with a leak valve, up to pressures of 10^{-6} Pa. Next, the gas phase was pumped off before the LEED experiments were carried out. The background pressure was then $\sim 10^{-8}$ Pa. Next the thermal desorption has been performed, and in this way the coverages have been determined.

First, we examined the volume-dominated case by the calculation of K'_{gs} with constant pressure $p = p^{(e)}$. As a result, a very large slope of the uptake curve was obtained, indicating that this is not the volume-dominated experimental setup. However, the solid-dominated version, having $\theta = \theta^{(e)}$, gave too small slope of the uptake curve. It was clear that this system represents an intermediate case, and some assumptions about the nonequilibrium pressure including the proportion between the volume of the chamber and the size of crystal surface have to be made.

For the calculation of the $\theta^{(e)}$ and $p^{(e)}$ as a function of nonequilibrium coverage and pressure, we used eq 12 rewritten to the following form:

$$\theta(t) + \frac{p(t)V}{MSkT} = \theta^{(e)} + \frac{p^{(e)}(\theta^{(e)})V}{MSkT} \quad (33)$$

where M is the number of surface substrate atoms ($M = 1.38 \times 10^{19}$ m^{-2} [43]) per unit of surface area, S is the geometrical area of the adsorbing surface, V is the volume of the chamber, and $p^{(e)}(\theta^{(e)})$ is the adsorption isotherm (eq 28). Unfortunately, the values of the quantities V and S have not been given in the description of the experimental procedure. So, we had to introduce a parameter, V/S, and to choose properly its value. If we assume that $S = 0.05$ cm^2 and $V = 5$ dm^3, the value of $V/S = 1000$ m. We cannot prove that these values of the parameters V and S are correct; probably they are not. Fortunately, the choice of the parameter V/S is not critical, and it can vary between 500 and 1500 m without changing much the calculated theoretical uptake curve.

The pressure during the adsorption of CO on Rh(100) cannot be considered as constant because it depends on the efficiency of the leak valve, on the difference between the actual and final equilibrium pressure, and particularly on the adsorption rate, that is, the rate of removal of CO molecules from the gas phase caused by their adsorption. We can write the following equation describing the pressure rise in the chamber:

$$\frac{dp}{dt} = \phi(p_0 - p) - \frac{MSkT}{V}\frac{d\theta}{dt} \quad (34)$$

where p_0 is the pressure up to which the chamber is back-filled and ϕ is the constant parameter that describes the efficiency of the leak valve. Its value must be suitably chosen for the assumed value of V/S to get a good match between the experimental and theoretical uptake curve. For the initial time, the pressure $p(0)$ is equal to background pressure, that is, 2×10^{-8} Pa.

Figure 10 shows the result of calculation of the uptake curve, using eqs 30−34. The original exposure scale was converted to the more convenient time scale, assuming that under the pressure 10^{-6} Pa, 1 L = 133 s. The value of the parameter ϕ was estimated to be 0.56 s^{-1} when V/S was assumed to be 1000 m. De Jong and Niematsverdriet reported that the value of the parameter p_0, that is, the pressure under which the kinetics was measured, was 10^{-6} Pa. However, it was necessary to assume a slightly higher value of this parameter, that is, 2×10^{-6} Pa.

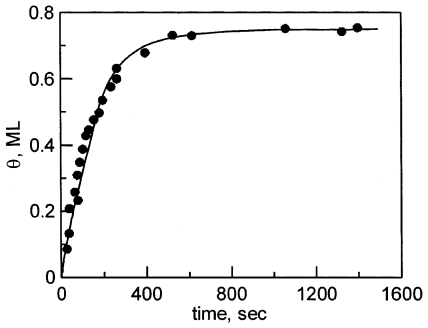

Figure 10. The result of fitting of eq 30 to the experimental data of the adsorption kinetics of CO on Rh(100). The original exposure scale was converted to time scale, assuming that 1 L = 133 s under the pressure 10^{-6} Pa.

It is not clear that value of $p_0 = 10^{-6}$ Pa as reported by de Jong and Niemantsverdriet is fully exact because the authors wrote that the calibration of their pressure meter is not accurately known.[42]

While calculating the theoretical uptake curve shown in Figure 10, we had to optimize, in fact, only one parameter, ϕ, because the other parameters in eq 30 were estimated while fitting the isosteric heat of adsorption. Of course, we had also to assume a certain value of the parameter *V*/*S*, but it was accepted on rational basis. As it was already mentioned, its value may be changed to some extent and equally good fit will be obtained, provided that we optimize the value of the parameter ϕ.

The application of the SRT to analyze the adsorption kinetics needs a detailed knowledge about the experimental conditions at which the process is carried out. Moreover, it needs also information about a temporal pressure change during adsorption. For this reason, the best way of realization of experiment would be a simultaneous monitoring of the coverage and the temporal pressure in the adsorption chamber. Then, one could avoid introduction of the parameter ϕ. However, the pressure change in the chamber during adsorption may be immeasurable because of extremely low pressures applied in chemisorption studies.

De Jong and Niemantsverdriet have obtained an equally good fit of the uptake curve as that presented in Figure 10. They used for the calculation a kinetic equation of the Kisliuk type

$$\frac{d\theta}{dt} \approx p_{CO}\frac{1-\theta}{1+(K_K-1)\theta} \tag{35}$$

and they came to the conclusion that adsorption kinetics of CO on Rh(100) can be described with the precursor model of Kisliuk.[2] However, we stress that the adsorption kinetics of CO on Rh(100) can be correctly described using the SRT without assuming the existence of a precursor state. Moreover, Kisliuk's equation (eq 35) does not account for the existence of the interactions between adsorbed molecules. Using eq 35, one assumes that the interactions do not play any role during adsorption and they start to play a significant role at equilibrium. The SRT approach takes into account correctly the existence of interactions between adsorbed molecules at equilibrium and during the kinetics as well.

Figure 11 presents the dependence of the nonequilibrium pressure p and the equilibrium coverage $\theta^{(e)}$ on the nonequilibrium coverage θ. When the leak valve is open, the pressure in the chamber rapidly rises from its background value up to 1.6×10^{-6} Pa; the coverage is then equal to about 0.05 ML. This process lasts a few seconds. Next, the pressure rises more slowly because the adsorption removes some part of CO molecules from the chamber. At the same time, also the difference between actual and final pressure becomes smaller.

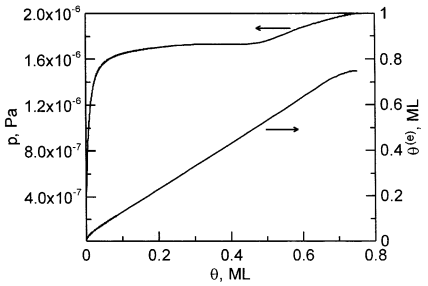

Figure 11. The changes of the nonequilibrium pressure and the equilibrium coverage as a function of the nonequilibrium coverage during the adsorption of CO on Rh(100).

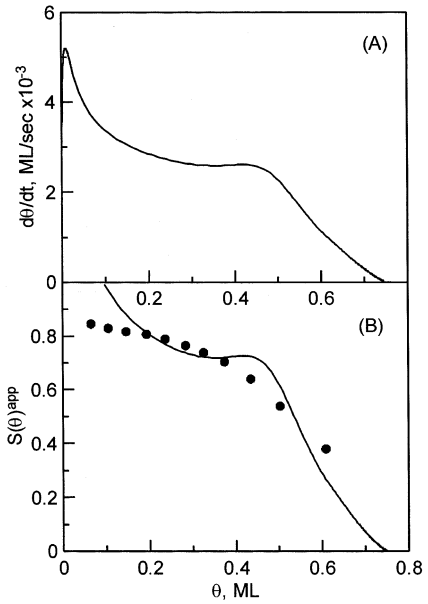

Figure 12. The changes (A) of the rate of adsorption with increasing surface coverage and the comparison (B) between sticking probability data reported by Kose et al. (●)[43] and the apparent sticking probability calculated from the fitting of the uptake curve reported by de Jong and Niemantsverdriet[42] using SRT eq 30.

The dependence between equilibrium coverage and nonequilibrium coverage calculated from eq 33 indicates that the system is similar to the solid-dominated one; however, a closer analysis shows that the θ and $\theta^{(e)}$ differ from each other for every value of θ.

In the last Figure 12, we show the dependence of rate of adsorption on the coverage θ. The $d\theta/dt$ is closely related to the sticking probability, but its exact calculation needs a detailed knowledge about incoming flux of the adsorbing molecules onto the surface. In part B of Figure 12, the apparent sticking coefficient is plotted versus coverage. We use the term "apparent sticking coefficient" because its calculation is based on the assumption that the flux of the CO molecules entering onto the surface of Rh can be expressed using the following equation:

$$F = \frac{p(\theta)}{\sqrt{2\pi(m_1+m_2)kT}} \tag{36}$$

where $p(\theta)$ is the nonequilibrium pressure plotted in Figure 11. Thus, the apparent sticking coefficient is defined as follows:

$$S(\theta)^{app} = \frac{d\theta/dt}{F} \tag{37}$$

The true flux of the CO molecules cannot be, however, calculated from eq 36 because this equation is correct only for a gas with a thermal velocity distribution, that is, the ideal gas under equilibrium. Because the pressure of CO changes rapidly for small surface coverages, the velocity distribution of CO molecules cannot be Maxwellian. For higher coverages, the changes in pressure are smaller and eq 36 can probably be applied. This is why the apparent sticking coefficient exceeds unity for small surface coverages. This nonphysical result is caused by too small value of the flux, F, generated by the eq 36.

The behavior of $d\theta/dt$ is also interesting; first, it takes very low values because of low pressure at initial time; next, it grows rapidly as a result of increasing pressure. It reaches a maximum and next falls down and seems to have a pseudo-platteau. The experimental sticking probability data reported by Kose et al.[43] indicate rather monotonic decrease of the sticking coefficient with increasing coverage, but up to 0.4 ML, this decrease is small.

Part B of Figure 12 does not represent a fit; it is prepared only for illustration because a real sticking coefficient cannot be properly calculated. For higher coverages, the sticking probability calculated from eq 37 is probably correct, but for this region of coverages, the experimental data are uncertain. The experimental values of $S(\theta)$ do not tend to zero at saturation, and Kose et al.[43] call it "steady state sticking coefficient". So, our sticking coefficient calculated on the basis of the uptake curve cannot be directly compared to the experimental values obtained using the pulsed molecular beam technique.

Generally, the statistical rate theory approach in the volume-dominated version predicts that the sticking probability should be proportional to $(1 - \theta)/\theta$, contrary to the ART approach in which $S(\theta) \approx (1 - \theta)$ for molecular adsorption. So, for small coverages, sticking coefficient calculated on the basis of the SRT will be higher than that calculated using the ART approach. Next, for coverages higher than 0.5 ML, $S(\theta)$ will decrease faster for the SRT approach. The decrease of $S(\theta)$ in the ART approach is caused by decreasing number of empty adsorption sites on the surface. In the SRT approach, it has a different source because the dependence on coverage is introduced via the chemical potential of adsorbed molecules. At a given surface coverage, the chemical potential has a certain value, no matter what was the past of the system. Such certain value of θ can be obtained in many different ways, including migration of the molecule over the surface when it strikes an already occupied site or surface diffusion of molecules to reach a more energetically favorable configuration. So, in the SRT approach it is not necessary that a molecule must strike an empty adsorption site to be adsorbed or to have enough energy to cross the local activation barrier. It resembles, to some extent, the mechanism of precursor-mediated adsorption, which was introduced as a modification of fundamentals of the ART approach by Kisliuk.[2]

For small values of θ, the term $(1 - \theta)/\theta$ would give very large values of the rate of adsorption; particularly, when $\theta = 0$, it would be infinite. However, the limit $\theta \rightarrow 0$ should be considered using a more fundamental expression than eq 3.[23] One can prove that when the number of adsorbed molecules tends to zero the rate of adsorption is not infinite but of course it is very large. In fact, the rate of adsorption for small values of θ is not very large, because it depends also on the nonequilibrium pressure, p. Even when the applied nonequilibrium pressure is high, it drops to small values in the surrounding of the adsorbing surface as a result of fast adsorption in the first stage of the process.

Summary

The statistical rate theory is based on thermodynamic fundamentals, and the existence of interactions between adsorbed molecules can easily be implemented in the theory. It correctly takes into account the possibility of interactions between incoming molecules with those already adsorbed. The shape of the sticking probability curve calculated on the basis of the SRT is nonlinear, and it takes higher values than those predicted by the ART approach for small coverages. On the basis of the SRT, it is not necessary to introduce the precursor state model; however, it does not exclude its existence.

The SRT approach needs a careful analysis of the experimental conditions at which the kinetics is measured. Particularly, it involves a detailed distinction between nonequilibrium and equilibrium pressure and coverage.

Acknowledgment. The authors express their thanks and gratitude to the Polish Foundation for Science (FNP) for the Grants for Young Scientists.

References and Notes

(1) Clark, C. A *The Theory of Adsorption and Catalysis*; Academic Press: New York, 1970.
(2) Kisliuk, P. *J. Phys. Chem. Solids* **1957**, *3*, 95.
(3) King, D. A. *Surf. Sci.* **1977**, *64*, 43.
(4) Gorte, R.; Schmidt, L. D. *Surf. Sci*. **1978**, *76*, 559.
(5) de Boer, J. H. *Adv. Catal*. **1956**, *8*, 1.
(6) Nagai, K. *Phys. Rev. Lett.* **1985**, *54*, 2159.
(7) Nagai, K.; Hirashima, A. *Chem. Phys. Lett.* **1985**, *118*, 401.
(8) Kreuzer, H. J.; Payne, S. H. Thermal Desorption Kinetics. In *Dynamics of Gas−Surface Interactions*; Rettner, C. T., Ashfold, M. N. R., Eds.; The Royal Society of Chemistry, Thomas Graham House, Science Park: Cambridge, U.K., 1991; p 221.
(9) Kreuzer, H. J.; Payne, S. H. Theories of Adsorption−Desorption Kinetics on Homogeneous Surfaces. In *Equilibria and Dynamics of Gas Adsorption on Heterogeneous Solid Surfaces*; Rudzinski, W., Steele, W. A., Zgrablich, G., Eds.; Elsevier: Amsterdam, 1997.
(10) Ward, C. A. *J. Chem. Phys.* **1977**, *67*, 229.
(11) Findlay, R. D.; Ward, C. A. *J. Chem. Phys*. **1982**, *76*, 5624.
(12) Rudzinski, W., Panczyk, T. *Adsorption* **2002**, *8*, 23.
(13) Ward, C. A.; Rizk, M.; Tucker, A. S. *J. Chem. Phys.* **1982**, *76*, 5606.
(14) Ward, C. A.; Tikuisis, P.; Tucker, A. S. *J. Colloid Interface Sci*. **1986**, *113*, 388.
(15) Tikuisis P.; Ward, C. A. In *Transport Processes in Bubbles, Drops and Particles*; Chabra, R., DeKee, D., Eds.; Hemisphere: New York, 1992; p 114.
(16) Ward, C. A.; Farabakhsk, B.; Venter, R. D. *Z. Phys. Chem.* **1986**, *147*, 89.
(17) Ward, C. A. *J. Chem. Phys.* **1983**, *79*, 5605.
(18) Skinner, F. K.; Ward, C. A.; Bardakjian, B. L. *Biophys. J*. **1993**, *65*, 618.
(19) Ward, C. A.; Findlay, R. D.; Rizk, M. *J. Chem. Phys*. **1982**, *76*, 5599.
(20) Ward, C. A.; Findlay, R. D. *J. Chem. Phys*. **1982**, *76*, 5615.
(21) Ward, C. A.; Elmoseli, M. B. *Surf. Sci*. **1986**, *176*, 457.
(22) Elliott, J. A. W.; Ward, C. A. *Langmuir* **1997**, *13*, 951.
(23) Elliott, J. A. W.; Ward, C. A. In *Equilibria and Dynamics of Gas Adsorption on Heterogeneous Solid Surfaces*; Rudzinski, W., Steele, W. A., Zgrablich, G., Eds.; Elsevier: New York, 1997.
(24) Elliott, J. A. W.; Ward, C. A. *J. Chem. Phys.* **1997**, *106*, 5677.
(25) Elliott, J. A. W.; Ward, C. A. *J. Chem. Phys*. **1997**, *106*, 5667.
(26) Dejmek, M.; Ward, C. A. *J. Chem. Phys*. **1998**, *108*, 8698.
(27) Ward, C. A.; Fang, G. *Phys. Rev. E* **1999,** *59*, 429.
(28) Fang, G.; Ward, C. A. *Phys. Rev. E* **1999**, *59*, 441.
(29) Fang, G.; Ward, C. A. *Phys. Rev. E* **1999**, *59*, 417.
(30) Rudzinski, W.; Borowiecki, T.; Dominko, A.; Panczyk, T. *Langmuir* **1997**, *13*, 3445.
(31) Rudzinski, W.; Borowiecki, T.; Dominko, A.; Panczyk, T.; Gryglicki, J. *Pol. J. Chem.* **1998**, *72*, 2103.
(32) Rudzinski W.; Panczyk, T. Surface Heterogeneity Effects on Adsorption Equilibria and Kinetics: Rationalisation of Elovich Equation. In *Surfaces of Nanoparticles and Porous Materials*; Schwarz, J., Contescu, C., Eds.; Marcel Dekker: New York, 1999.
(33) Rudzinski, W.; Borowiecki, T.; Dominko, A.; Panczyk, T. *Langmuir* **1999**, *15*, 6386.

(34) Rudzinski, W.; Borowiecki, T.; Panczyk, T.; Dominko, A. *J. Phys. Chem. B* **2000**, *104*, 1984.
(35) Rudzinski, W.; Panczyk, T. *J. Phys. Chem. B* **2000**, *104*, 9149.
(36) Rudzinski, W.; Borowiecki, T.; Panczyk, T.; Dominko, A. *Langmuir* **2000**, *16*, 8037.
(37) Rudzinski, W., Panczyk, T. *J. Phys. Chem. B* **2001**, *105*, 6858.
(38) Rudzinski, W., Panczyk, T. *Langmuir* **2002**, *18*, 439.
(39) Rudzinski, W.; Borowiecki, T.; Panczyk, T.; Dominko, A. *Appl. Catal., A* **2002**, *224*, 299.
(40) Hill, T. L. *An Introduction to Statistical Thermodynamics*; Dover Publications Inc.: New York, 1986.
(41) Ceyrolles, W. J.; Viot, P.; Talbot, J. *Langmuir* **2002**, *18*, 1112.
(42) de Jong, A. M., Niemantsverdriet, J. W. *J. Chem. Phys.* **1994**, *101*, 10126.
(43) Kose, R.; Brown, W. A.; King, D. A. *J. Phys. Chem. B* **1999**, *103*, 8722.
(44) Baraldi, A.; Gregoratti, L.; Comelli, G.; Dhanak, V. R.; Kiskinova, M.; Rosei, R. *Appl. Surf. Sci.* **1996**, *99*, 1.
(45) Kim, Y.; Peebles, H. C.; White, J. M. *Surf. Sci.* **1982**, *114*, 363.
(46) Wei, D. H.; Skelton, D. C.; Kevan, S. D. *Surf. Sci.* **1997**, *381*, 49.